Reverse energy-pooling collisions: $K(5D)+Na(3S)\rightarrow K(4P)+Na(3P)$

S. Guldberg-Kjær, G. De Filippo, S. Milošević,* S. Magnier,† and J.O.P. Pedersen
Niels Bohr Institute, Ørsted Laboratory, Universitetsparken 5, DK-2100, Copenhagen Ø, Denmark

M. Allegrini‡
Unità INFM, Dipartimento di Fisica, Università di Pisa, Piazza Torricelli 2, I–56126, Pisa, Italy
(Received 23 August 1996; revised manuscript received 2 December 1996)

The observation of a heteronuclear reverse energy pooling process is reported. The cross section for the collision processes $K(5D)+Na(3S)\rightarrow K(4P)+Na(3P)$ has been measured and compared to calculations carried out using a multicrossing Landau-Zener model. [S1050-2947(97)50204-6]

PACS number(s): 34.50.Rk, 34.10.+x, 34.90.+q

Energy pooling (EP) is a process where two excited atoms collide and produce one highly excited atom and one ground-state atom [1]. Typically optical excitation is used to prepare the colliding partners in the excited state, and the highly excited atoms, populated by the EP collisions, are detected through their fluorescence. The process has been extensively studied in alkali-metal vapors for both homonuclear [2] and heteronuclear collisions [3–5], whereas studies of the reverse process are almost nonexisting. In reverse energy pooling (REP) an atom prepared in a highly excited state collides with an atom in the ground state, and the result of the collision is two excited atoms. The process was observed by Yabuzaki *et al.* [6] in Cs vapor, preparing the initial state as a result of a stepwise laser excitation via the Cs_2 dimer. For experiments dealing only with atomic levels, the identification of the REP by fluorescence detection in a homonuclear system is complicated by radiative decay of the optically excited atom in the entrance channel. A heteronuclear system, on the contrary, offers the advantage that we can measure the fluorescence of the atomic species not directly prepared by the laser excitation.

In this Rapid Communication we present a combined experimental and theoretical study of REP collisions

$$K(5D_J)+Na(3S_J) \xrightarrow{k_{3P_J}} K(4P_J)+Na(3P_J), \quad (1)$$

where k_{3P_J} indicates the REP rate coefficients.

This is a study of reverse EP processes in a heteronuclear system and of REP with the atomic initial state directly prepared. The (forward) EP process, $K(4P)+Na(3P)$, has already been observed [3] and the cross sections have been measured [4] for the exothermic $K(4S)+Na(3D)$ and the endothermic $K(5D)+Na(3S)$ and $K(7S)+Na(3S)$ exit channels. [Note that the values in [4] must be corrected by a factor of 2, because they were measured relative to a homonuclear pooling process, which must be corrected [7] to avoid double counting of atom pairs.] The REP cross section cannot be easily calculated from the direct EP cross section using the principle of detailed energy balance, because of the large number of open exit channels. For example, in addition to the four investigated $K(4P_J)+Na(3P_J)$ exit channels [exothermic by (169–244) cm^{-1}], other exit channels, such as $K(4S_J)+Na(4P_J)$ (endothermic by 81 cm^{-1}) and $K(7S)+Na(3S)$ (endothermic by 89 cm^{-1}), are possible.

In the present experiment we use two broadband cw dye lasers to excite the $K(5D)$ level in two steps, as sketched in Fig. 1, in a mixture of Na and K (alloy of 95% Na and 5% K) contained in a capillary cell of 1.8 mm diameter sealed under vacuum. This composition gives approximately the same ground-state Na- and K-atom densities in the vapor mixture at 470 K. The use of a capillary cell minimizes radiation trapping, and assures a good overlap of the two laser beams and a uniform filling of the cell body [8]. For the two-step excitation of the $K(5D)$ level, the first laser is tuned to the 769.9-nm $K(4S_{1/2}\rightarrow 4P_{1/2})$ transition and the second to the 583.2-nm $K(4P_{3/2}\rightarrow 5D_{5/2})$ transition because this is the combination that gives the best signal-to-noise ratio in our experiment. The fluorescence is directed into a 0.67-m monochromator equipped with a R943-02 Hamamatsu pho-

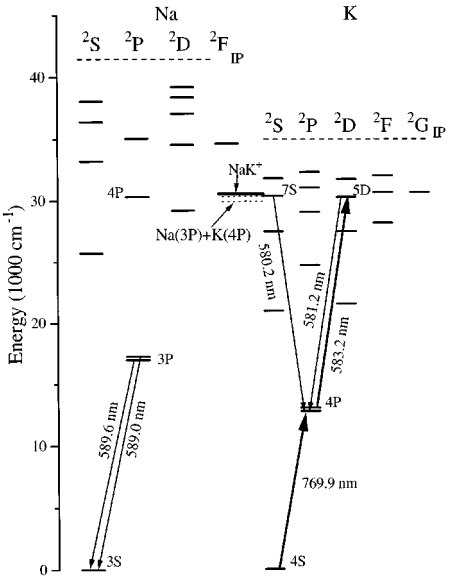

FIG. 1. Sketch of the excitation and observation scheme. The energy of the exit channel is shown by the dotted line.

*Permanent address: Institute of Physics, HR-10000 Zagreb, Croatia.

†Present address: Technopole 2000, Laboratoire IPCM, F-57000 Metz, France.

‡Also at Dipartimento di Fisica della Materia e Tecnologie Fisiche Avanzate, Università di Messina, I-98166 Messina, Italy.

 © 1997 The American Physical Society

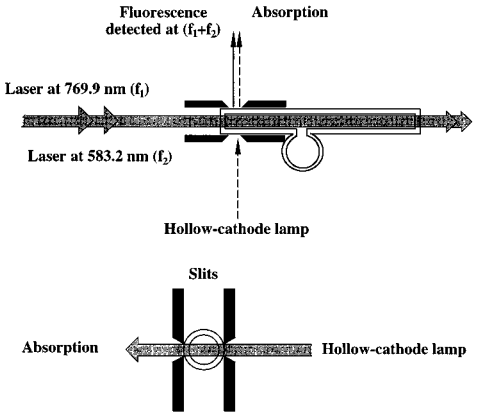

FIG. 2. Schematic of the experimental setup.

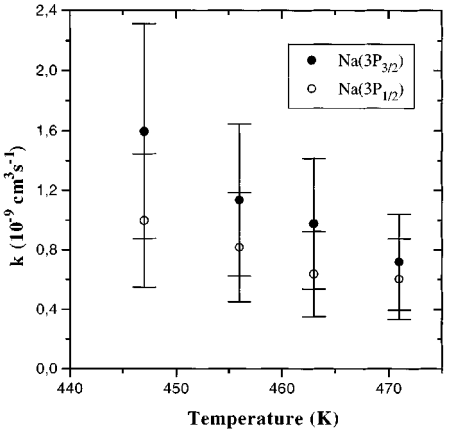

FIG. 3. The rate coefficients $k_{3P_{3/2}}$ for the Na($3P_{3/2}$) (filled circles) and $k_{3P_{1/2}}$ for the Na($3P_{1/2}$) (open circles) exit channels.

tomultiplier. The volume from which fluorescence is observed is restricted by rectangular slits of size 0.8×1.5 mm^2 (Fig. 2). The two laser beams are merged at a small angle and chopped at two different and incommensurable frequencies, f_1 and f_2, and the fluorescence signals are recorded at the sum frequency (f_1+f_2) using a lock-in amplifier. Thus, in principle, only the contributions to the spectrum due to K($5D$)$+M$ collisions (cf. Ref. [5]) are recorded, where M is an atomic species present in the cell. Perpendicular to the direction of the laser beam, the fluorescence volume is crossed by the light from a hollow-cathode Na-K lamp. The absorption of the 589.0- and the 769.9-nm Na and K atomic lines are used to determine the ground-state densities. To calculate the absorption cross sections for the Doppler-broadened transitions, we have used the natural radiative rates $\Gamma_{3P_{3/2}\rightarrow3S_{1/2}}=6.10\times10^7$ s^{-1} [9] and $\Gamma_{4P_{1/2}\rightarrow4S_{1/2}}=3.82\times10^7$ s^{-1} [10] for Na and K, respectively. The density measurements have confirmed that the densities of the two atomic species in the vapor phase were approximately the same and in the range $(0.8–2.0)\times10^{12}$ cm^{-3} for our temperatures. The relative sensitivity of the detection system was measured by passing the light from a calibrated halogen lamp through the cell. The detection system is sensitive from ~400 to ~850 nm, but outside this range the sensitivity decreases rapidly.

The temperature of the cell was varied between 446 and 471 K, and for each temperature the intensities of the lines at 581.2 nm [K($5D_{3/2}\rightarrow4P_{1/2}$)], 580.2 nm [K($7S_{1/2}\rightarrow4P_{3/2}$)], 589.0 nm [Na($3P_{3/2}\rightarrow3S_{1/2}$)], and 589.6 nm [Na($3P_{1/2}\rightarrow3S_{1/2}$)] were measured by scanning the monochromator over the region 579.5–581.5 nm and 588.0–590.0 nm. The measured line shapes were fitted by Gaussian curves of fixed halfwidth. This allowed us to subtract a linear background that was found to be approximately 10% of the maximum measured intensities. The background may be due to the limited dynamic reserve of the lock-in amplifier and to signals at the sum frequency. These may be due to laser broadband emission (amplified stimulated emission) and to scattering from the capillary cell.

Simplified steady-state rate equations for the population of Na($3P_J$) levels are given as

$$-\Gamma_{3P_J-3S}[\mathrm{Na}]_{3P_J}+k_{3P_J}[\mathrm{K}]_{5D}[\mathrm{Na}]_{3S}=0. \qquad (2)$$

We have assumed that the main depopulation mechanism of the Na($3P_J$) state is radiation towards the ground state, and we have neglected other mechanisms populating Na($3P_J$). Fine-structure mixing of the Na($3P_{1/2,3/2}$) levels due to collisions with Na and K can be safely neglected, even at our maximum ground-state atom densities of 10^{12} cm^{-3}, according to measured cross sections [11,12]. In particular, we have neglected cascade from higher-lying levels of Na [particularly Na($4P$)], which may also be populated by the K($5D$)+Na collisions or as a product of ionization and recombination. Unfortunately, we were not able to observe the transitions Na($4P\rightarrow3S$) at 330 nm or Na($4P\rightarrow4S$) at 1.14 μm because of the very low spectral response of our optical system at these wavelengths. The system is, however, sensitive at 818.3 nm (with a relative response of 0.1 compared to 589 nm), and we have not observed the cascade emission Na($3D\rightarrow3P$). From the background level in our spectra and the spectral response, we estimate that we would be able to observe the Na($3D\rightarrow3P$) transition if the intensity were larger than 10% of the Na($3P\rightarrow3S$) transition. Thus we conclude that the cascade from Na(nl) states with $n,\ l\geqslant3$ contributes less than 10% to our signal. We further note that due to the large $(120\times10^{-16}$ cm$^2)$ cross section for Na($4P$)+Na($3S$)$\rightarrow$Na($3D$)+Na($3S$) process [13] the missing Na($3D\rightarrow3P$) transition leads to the conclusion that the Na($4P$) level is not significantly populated in the present experiment. This conclusion is also supported by our theoretical prediction of the cross section for the process K($5D$)+Na($3S$)$\rightarrow$K($4S$)+Na($4P$). As shown below, this amounts to 37×10^{-16} cm^2 at 470 K, or less than 20% of the title reaction. Depending on the considered J level, the contribution to the Na($3P$) population is 20–40 % of the role for this process, and we thus estimate the total contribution to our signal to be less than 10%. A possible increase of the Na($3P$) population due to the production of K($7S$) in the K($5D$)$+M$ collisions, which, followed by a REP process similar to (1), leads to Na($3P$)+K($4P$), is found to contribute less than 8% from analysis of the measured fluorescence intensity $[(I_{7S-4P})/(I_{5D-4P})]$ ratio. Another contribution to the Na($3P$) signal may be due to recombination of produced ions (NaK^+, Na_2^+, Na^+) followed by cascade. However, the energy of the most favorable ionization channel, i.e., $NaK^+ + e^-$, is endothermic by 230 ± 1 cm^{-1} [14] and thus expected to be small compared with the exothermic REP process (1). If a significant number of NaK^+ were produced, we would also expect highly excited states of Na to be popu-

TABLE I. Cross sections for energy-pooling and reverse energy-pooling collisions in NaK.

Process	σ (10^{-16} cm^2)	T (K)	Reference
$K(4P)+Na(3P)\rightarrow K(4S)+Na(3D)$	28 ± 14	513	[4]
$K(4P)+Na(3P)\rightarrow K(5D)+Na(3S)$	38 ± 19	513	[4]
$K(4P)+Na(3P)\rightarrow K(7S)+Na(3S)$	18 ± 9	513	[4]
$K(5D)+Na(3S)\rightarrow K(4P_J)+Na(3P_{1/2})$	95 ± 45	465	This work, experiment
$K(5D)+Na(3S)\rightarrow K(4P_J)+Na(3P_{3/2})$	125 ± 55	465	This work, experiment
$K(5D)+Na(3S)\rightarrow K(4P)+Na(3P)$	220 ± 100	465	This work, experiment
$K(5D)+Na(3S)\rightarrow K(4P)+Na(3P)$	400	465	This work, calculation
$K(5D)+Na(3S)\rightarrow K(4S)+Na(4P)$	37	465	This work, calculation

lated from dissociative recombination of NaK^+. Unfortunately, our sealed cells cannot be easily modified to detect ions, and therefore a direct check of the presence of NaK^+ has not been possible in the present experiment. However, the missing $Na(3D\rightarrow3P)$ emission indicates that the population of higher excited levels in Na can be neglected when compared with process (1). Moreover, typical associative ionization cross sections in alkali metals are of the order 10^{-17} cm^2 [15], indicating a process less effective than the reverse energy pooling we have observed. Since the cell is fully illuminated by the laser, we expect the spatial distribution of $K(5D)$ to be isotropic. However, since the size of the radiative lifetime, the average time between collisions, and the diffusion time for the $K(5D)$ atoms are all of the same magnitude, diffusion of the $K(5D)$ has to be considered. The intensity of the $K(5D\rightarrow4P)$ line decreases because of the losses from collisions with the cell walls. However, the same losses also reduce the production of $Na(3P)$ by the same fraction. Adding the various possible contributions to the Na $(3P)$ signal discussed above, we find them to be less than 25%.

In terms of the measured fluorescence intensities I, we obtain

$$k_{3P_J}=\alpha\left(\frac{I_{3P_J-3S}}{I_{5D_{3/2}-4P_{1/2}}}\right)\frac{\nu_{5D_{3/2}-4P_{1/2}}\Gamma_{5D_{3/2}-4P_{1/2}}}{\nu_{3P_J-3S}}\frac{1}{[\mathrm{Na}]_{3S}}, \tag{3}$$

where the intensity ratio is corrected for the spectral response of our apparatus, and $\Gamma_{5D_{3/2}-4P_{1/2}}$ is the effective radiation rate that we have calculated in the presence of radiation trapping starting from the natural value [16]. The factor α arises from the fact that measured radiation at 581.2 nm does not account for the total $K(5D_J)$ level population. Under the assumption of thermal redistribution between $K(5D_{3/2})$ and $K(5D_{5/2})$ levels we obtain $\alpha\approx2/5$. Following the discussion above we do not correct the ratio for diffusion effects. We see that we have to measure the relevant intensity ratios as well as the sodium ground-state atom density.

The experimental results are shown in Fig. 3 and give an averaged value of $k_{3P_{3/2}}=1.1\times10^{-9}$ cm^3 s^{-1} and $k_{3P_{1/2}}=0.8\times10^{-9}$ cm^3 s^{-1} at $T=460$ K. The uncertainties on the fluorescence ratios ($\sim$25%) were determined by performing several independent measurements. The uncertainty in density measurements is $\sim$15% mainly due to the uncertainty of the temperature measurement. From a comparison of the available literature's data on $\Gamma_{5D_{3/2}\rightarrow4P_{1/2}}$ we have found that this rate has an uncertainty of $\sim$20%. In addition, various other systematic effects and uncertainties should be considered, and as mentioned above, the rates could include a 25% contribution from other processes. Adding in quadrature, we obtain an overall uncertainty of $\sim$45%.

We note that each of the rate coefficients $k_{3P_{3/2}}$ and $k_{3P_{1/2}}$ is a sum of the two exit channels related to $K(4P_{3/2})$ and $K(4P_{1/2})$, which are not separated in the experiment. We also note that both rate coefficients are decreasing with increasing temperature, with $k_{3P_{3/2}}$ showing the fastest change. At the lowest temperature we find that the ratio between $k_{3P_{3/2}}$ and $k_{3P_{1/2}}$ is approximately 2, but at the highest temperature both rate coefficients give the same value of approximately 0.7×10^{-9} cm^3 s^{-1}.

Several effects can cause the decrease of the rate coefficients with increasing temperature, such as the radiation trapping, a J dependence on the entrance and exit channels, or a strong $3P_J$ depopulation by some other collisional process. We can exclude here the radiation trapping by the following consideration. First we note that the rate coefficient does not depend on the $\Gamma_{3P_J-3S_{1/2}}$, which could be affected by radiation trapping. As seen from Eq. (3) both components depend only on $\Gamma_{5D_{3/2}\rightarrow4P_{1/2}}$. The effect of the radiation trapping for this transition has been calculated by assuming the maximum possible $K(4P)$ density, namely under the conditions of a saturated transition in the first step of the excitation scheme $[K(4P)\approx\frac{2}{3}K(4S)]$, and using the theory of Molisch for an infinite cylinder [17]. We have found that radiation trapping is negligible under present experimental conditions for the $K(5D_{3/2}\rightarrow4P_{1/2})$ transition. The relative change of $K(5D_{3/2})$ and $K(5D_{5/2})$ populations versus temperature is unlikely since the energy difference between these two levels is only 0.51 cm^{-1}. In Table I we show relevant velocity-

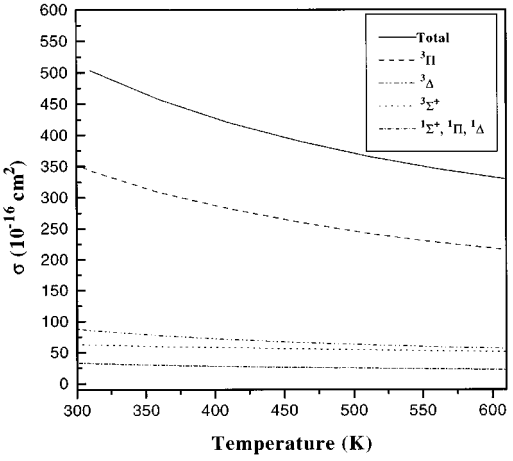

FIG. 4. The calculated cross sections for different symmetries in the temperature range 350–600 K. The total cross section is shown by the solid line.

averaged cross sections σ given by the relation $\sigma = k/v$, where $v = \sqrt{8k_B T/\pi M}$ is the interatomic velocity.

The theoretical cross section for the process (1) has been determined in the framework of a semiclassical multicrossing Landau-Zener (LZ) model developed for Na_2 [18]. In the present work, we have considered all adiabatic potential curves correlated from $K(4F)+Na(3S)$ up to $K(4S)+Na(4P)$ computed by a pseudopotential method [19] over a wide range of internuclear distances. We have extracted the relevant LZ parameters for the numerous avoided crossings, and at each pseudocrossing we have estimated the population transfer from one potential curve to another. Total cross sections have been determined by integrating numerically the final population of each possible exit channel over different impact parameters. Figure 4 shows results of the calculations for process (1) in the temperature interval 300-600 K for different symmetries. The major contribution comes from the avoided crossings of the $^3\Pi$ symmetry states.

In the experiment the atom densities were sufficiently low for the fine-structure mixing collisions $Na_{3P_{3/2}\leftrightarrow 3P_{1/2}}$ and $K_{4P_{3/2}\leftrightarrow 4P_{1/2}}$ to be neglected, as shown in the work of Davidson *et al.* [20]. Therefore, the experimental cross sections are sensitive to the different J sublevels, whereas the theoretical treatment does not include the fine-structure interaction in the calculation of the potential-energy curves. For this reason we can only compare the theoretical results with the total experimental cross section for the reverse energy pooling obtained as we described above by summing the cross sections for the two exit channels.

We conclude that a reasonable agreement between theory and experiment exists within the combined uncertainties of the experiment and the semiclassical model. In the temperature interval 446–481 K, a total cross section of $(220\pm 100)\times 10^{-16}$ cm^2 is obtained and can be compared with the theoretical cross section of approximately 400×10^{-16} cm^2. The large cross section is not surprising compared to the earlier REP work on Cs [6], giving the value 150×10^{-16} cm^2, and our measured REP cross section also fits well into the set of measured cross-section values for EP (exothermic) processes (see Fig. 3 of Ref. [5]). We also note that, even though the model predicts some temperature dependence, the strong temperature dependence of the experimental cross sections is not reproduced by the model. However, the fact that the main contribution to the calculated cross section comes from the avoided crossings of the $^3\Pi$ symmetry curve shows that the observed cross sections could be sensitive to the J selection of the entrance and exit channels. Taking the fine-structure splitting into account in the model will lead to more avoided crossings of the potential curves and possibly a better agreement with the experiment. If only one crossing were active, the strong temperature dependence would indicate a strong repulsion of the potential curves at the crossing point (cf. the discussion in [21]), or the decrease of the cross section with increasing temperature could indicate the opening of a competing endothermic exit channel. However, several crossings are probably involved and render a simple analysis impossible. We also stress that from the results of a similar comparison between the LZ model and experiment on energy pooling in the Na-Na system [21] we might only expect to reproduce the cross section within a factor of 2. Thus the experiment also indicates that the semiclassical approach is not sufficient and that very interesting dynamics are probably occurring in the experiment.

In conclusion, we have observed heteronuclear reverse energy pooling and have demonstrated that studies of the energy-pooling processes in both the forward and the reverse path raise interesting new questions for experiment and theory, such as the inclusion fine-structure splitting in the calculation for the cross sections, and an understanding of the J selectivity.

This work is supported by the Danish Natural Science Research Council, Ib Henriksens Foundation (Copenhagen), and by the EEC-HCM program (Grant No. ERBCHRXCT930344). We thank Nils Andersen for lending us most of the equipment used in the experiment and F. Masnou-Seeuws and Ph. Millié for several stimulating discussions. Finally we thank John Huennekens for useful comments on the manuscript.

[1] M. Allegrini *et al.*, Opt. Commun. **19**, 96 (1976).
[2] Z. J. Jabbour *et al.*, Phys. Rev. A **54**, 1372 (1996).
[3] M. Allegrini *et al.*, Opt. Commun. **36**, 445 (1981).
[4] S. Gozzini *et al.*, Opt. Commun. **63**, 97 (1987).
[5] C. Gabbanini *et al.*, Phys. Rev. A **39**, 6148 (1989).
[6] T. Yabuzaki *et al.*, Opt. Commun. **24**, 305 (1978).
[7] N. N. Bezuglov *et al.*, J. Phys. B **20**, 2497 (1987).
[8] M. Allegrini *et al.*, Phys. Rev. A **28**, 1338 (1983).
[9] A. Gaupp *et al.*, Phys. Rev. A **26**, 3351 (1982).
[10] *Atomic Transition Probabilities*, edited by W. L. Wiese *et al.*, Natl. Bur. Stand. Ref. Data Ser., Natl. Bur. Stand. (U.S.) Circ. No. 22 (U.S. GPO, Washington, DC, 1969), Vol. II.
[11] J. Huennekens and A. Gallagher, Phys. Rev. A **27**, 1851 (1983).
[12] V. Horvatic *et al.*, Z. Phys. D **34**, 163 (1995).
[13] S. Magnier *et al.*, Z. Phys. D. (to be published).
[14] S. Leutwyler *et al.*, Chem. Phys. Lett. **77**, 257 (1981).
[15] M. Allegrini *et al.*, J. Phys. (France) Colloq. **46**, C1-61 (1985).
[16] B. Warner, Mon. Not. R. Astron. Soc. **139**, 115 (1968).
[17] A. F. Molisch *et al.*, J. Quant. Spectrosc. Radiat. Transf. **49**, 361 (1993).
[18] I. Yu Yurova *et al.*, J. Phys. B **27**, 3659 (1994).
[19] S. Magnier and Ph. Millie *et al.*, Phys. Rev. A **54**, 204 (1996).
[20] S. A. Davidson *et al.*, Phys. Rev. A **33**, 3756 (1986).
[21] J. Brust and A. C. Gallagher, Phys. Rev. A **52**, 2120 (1995).